

Design to Improve Starting Capability of Single-Phase Line-Start Synchronous Reluctance Motor

Hyuk Nam¹, Su-Beom Park¹, Jung-Pyo Hong¹, Tae-Uk Jung², Jae-Boo Eom²

¹ Department of Electrical Engineering, Changwon National University

#9 Sarimdong, Changwon, Gyeongnam, 641-773, Korea, Tel: (+8255)2625966, Fax: (+8255) 2639956

² Research Laboratory, Digital Appliance Company, LG Electronics

#391-2 Gaeumjeongdong, Changwon, Gyeongnam, 641-711, Korea, Tel: (+8255)2603834, Fax: (+8255) 2603507

E-mail: haeggee@korea.com, jphong@changwon.ac.kr, tujung@lge.com, jbeom@lge.com

I. INTRODUCTION

A single-phase line-start synchronous reluctance motor (LSynRM) starts asynchronously by means of an induction cage and operates as a synchronous motor by flux barriers that cause the difference in d-axis inductance (L_d) and q-axis inductance (L_q) [1]. Since the motor operates as a synchronous machine in the steady-state, the rotor joule loss is significantly reduced [2]. Therefore, the LSynRM is capable of efficiency improvement without cost rise when compared with a single-phase induction motor (SPIM).

However, unless high saliency ratio (L_d/L_q) and high inductance difference (L_d-L_q) are reached, torque density, power factor, and efficiency are low in the steady-state [3].

For this reason, q-axis conductor bars should be reduced to obtain d-axis flux path sufficiently. In contrast, d-axis conductor bars should be increased to reduce the conductor bar loss by the unbalanced rotating magnetic field. With flux barriers, the different shape of the conductor bars can induce the unbalanced locking torque according to the initial starting position of the rotor. As a result, the LSynRM can have difficulty in starting according rotor positions

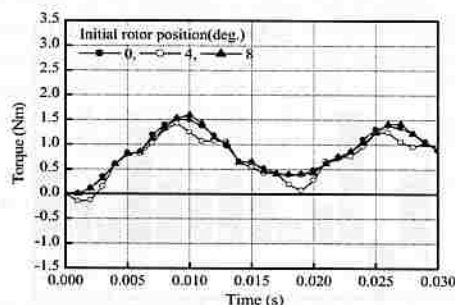
This paper deals with the LSynRM design to improve starting capability. Design variables are the number and the shape of the conductor bars.

Firstly, the number of the conductor bars is decided to be suitable for uniform locking torque. Secondly, locking torque characteristics are analyzed according to the shape of the bars. Then, the effect of the flux barriers is analyzed at 3 flux barriers. Lastly, the shape of the conductor bars is designed to satisfy the stable locking torque. A SPIM for mass production and a designed model of the LSynRM are manufactured and tested.

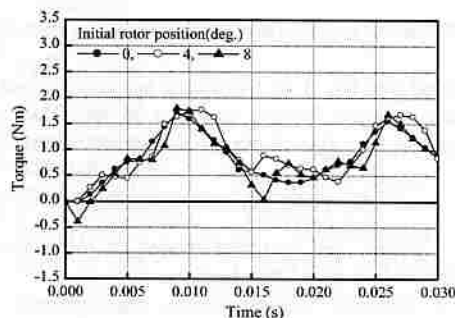
II. LSYNRM DESIGN PROCEDURE

A. Decision of the Number of the Conductor Bars

Fig. 1 shows the finite element (FE) analysis results of the locking torque. The analysis models do not have flux barriers. While the locking torque with 33 bars has almost uniform value, the torque variation with 34 bars is larger a little bit than that with 33 bars. In the case of the LSynRM, an even number of the conductor bars is suitable because the motor requires the symmetric magnetic circuit. Thus, the rotor of the LSynRM has 34 bars in this paper.



(a) 33



(b) 34

Fig. 1 Locking torque characteristics

B. Locking Torque with the Shape of the Bars

Fig. 2 presents the characteristic analysis model according to the shape of the bars. The model has 34 conductor bars and 3 flux barriers. D-axis and q-axis conductor bars are numbered from the center of d-axis and q-axis, respectively, in counterclockwise (CCW) direction. Flux barriers are numbered from the shaft in radial direction. In the figures, the initial rotor position is zero, which is an angle between the center of the main winding and the d-axis of the rotor.

When the shape of the bars varies in order, the motor does not have flux barriers. In other words, the motor operates as a SPIM. On the other hand, when the motor has flux barriers, conductor bars have equal shape.

Fig. 3 displays the average locking torque characteristics by FE analysis. "Ref" means the SPIM which has uniform conductor bars. "Bard", "Barq", and "Barr" mean the d-axis bar, the q-axis bar, and the flux barrier, respectively. The area of the changed bar is twice as large as that of the original bar

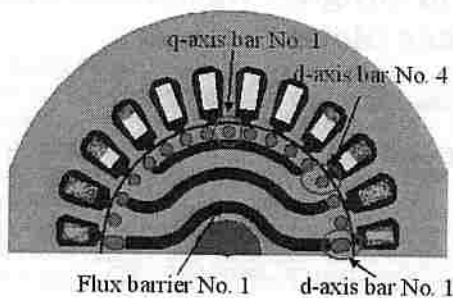


Fig. 2 Analysis models of the LSynRM.

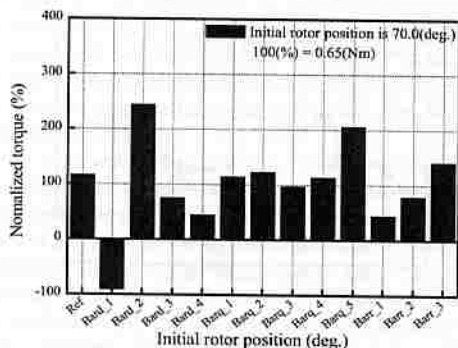


Fig. 3 Analysis results of average locking torque at 70 deg.

Provided that No. 1 of the d-axis bar is increased, the bar causes negative locking torque at 70 deg. The rest of the conductor bars also shows the similar characteristics.

III. EXPERIMENTAL RESULTS

Fig. 4 shows the designed model of the LSynRM, which has 34 bars and 3 flux barriers.

Fig. 5 indicates locking torque characteristics. The designed model generates positive locking torque all over the initial rotor position even though the locking torque between 20 deg. and 40 deg. is smaller than in other degrees.

Table I is the starting-state experimental results. In the table, the starting presents the period to reach synchronous speed after power is supplied. Furthermore, standard voltage means the voltage considering the maximum voltage drop when input voltage varies.

The designed model can be started in the cooling condition as well as standard and overload conditions near the rated voltage of 115 V.

Table II summarizes the steady-state experimental results of the compressor. The compressor efficiency of the designed model is increased by 2.7 % in comparison with the SPIM. It is because the rotor joule loss is significantly reduced.

IV. CONCLUSIONS

This paper deals with the LSynRM design to improve starting capability. The designed model can be started in cooling, standard, and overload conditions near the rated voltage of 115 V.

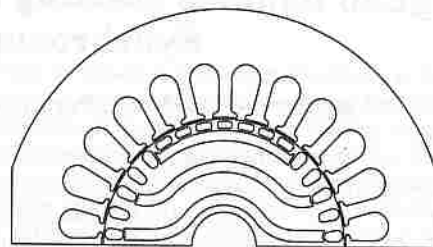


Fig. 4 Prototype and designed model of the LSynRM.

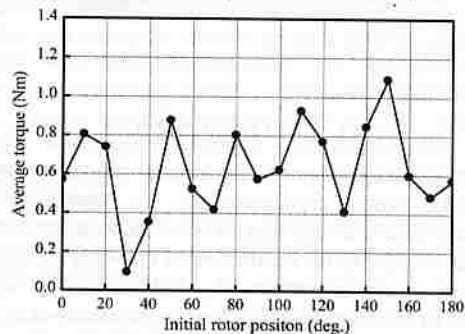


Fig. 5 Analysis results of average locking torque.

TABLE I. STARTING-STATE EXPERIMENTAL RESULTS.

Item	Unit	Standard	Designed model
Standard	V	97.7	107.0
Overload	V	103.5	108.0
Cooling	V	92.0	119.0

TABLE II. STEADY-STATE EXPERIMENTAL RESULTS.

Item	Unit	SPIM	Designed model
Torque	kgf-cm	22.1	22.8
Speed	rpm	3434	3600
Power factor	%	96.8	96.0
Efficiency	%	84.3	87.0
I st loss	W	62.0	82.0
Input power	W	925.9	966.2

However, the motor does not still satisfy the standard voltage range because the compressor is stopped near synchronous speed after induction starting.

It is analyzed that the maximum reluctance torque is not obtained sufficiently. To satisfy the starting condition, therefore, it is important to obtain the maximum reluctance torque as well as to accomplish the stable locking torque.

V. REFERENCES

- [1] H. Murakami, Y. Honda, H. Kiriya, S. Morimoto, and Y. Takeda, "The performance comparison of SPMSM, IPMSM and SynRM in use as air-conditioning compressor," in Conf. Rec. the 34th IAS Annual Meeting, vol. 2, pp. 840-845, Oct.1999.
- [2] A. M. Knight, and C.I. McClay, "The design of high-efficiency line-start motors," in Conf. Rec. the 34th IAS Annual Meeting, vol. 1, pp. 516-522, Oct.1999.
- [3] I. Boldea, Z. X. Fu, and S. A. Nasar, "Performance evaluation of axially-laminated anisotropic (ALA) rotor reluctance synchronous motors," IEEE Trans. Ind. Applicat., vol.30, no.4, pp. 977-985, July/August 2003.

Design to Improve Starting Capability of Single-Phase Line-start Synchronous Reluctance Motor

¹Hyuk Nam, ¹Su-Beom Park, ¹Jung-Pyo Hong, Senior Member, *IEEE*, ²Tae-Uk Jung, and ²Jae-Boo Eom

¹Department of Electrical Engineering, Changwon National University

#9 Sarimdong, Changwon, Gyeongnam, 641-773, Korea, phone: (+8255)2625966, fax: (+8255) 2639956

²Research Laboratory, Digital Appliance Company, LG Electronics

#391-2 Gaeumjeongdong, Changwon, Gyeongnam, 641-711, Korea, phone: (+8255)2603834, fax: (+8255) 2603507

e-mail: haeggee@korea.com, akdma00@hotmail.com, jphong@sarim.changwon.ac.kr, tujung@lge.com

Abstract— This paper presents the design to improve starting capability of a single-phase line-start synchronous reluctance motor (LSynRM). Design variables are the number and the shape of the conductor bars. The motor is analyzed by finite element method (FEM). The starting torque of a prototype and a designed model of the LSynRM are compared according to the initial starting position of the rotor.

I. INTRODUCTION

A single-phase line-start permanent magnet synchronous motor (LSPMSM) has both a rotor cage for induction starting and permanent magnets (PMs) for synchronous torque. Since the motor operates as a synchronous machine in the steady-state, the rotor joule loss is significantly reduced [1]

Therefore, it is possible to achieve efficiency improvement in comparison with a single-phase induction motor (SPIM). Yet the instantaneous starting current can lead the deterioration of motor performance as well as the irreversible demagnetization of PMs [2].

On the other hand, a single-phase line-start synchronous reluctance motor (LSynRM) has conductor bars and flux barriers in the rotor, and does not need PMs contrary to the LSPMSM.

With the help of an induction cage, as shown in Fig. 1, the motor starts asynchronously. When the motor reaches synchronous speed, the reluctance torque by flux barriers, which cause the difference in d-axis inductance (L_d) and q-axis inductance (L_q), becomes the sole source and operates as a synchronous motor in steady-state.

Accordingly, the LSynRM is capable of efficiency improvement without cost rise compared with the SPIM [3]. Most of all, the LSynRM can be independent to the demagnetization field, and the drop ratio in efficiency of the LSynRM is smaller than that of the LSPMSM. Therefore, the LSynRM can improve the reliability contrary to the LSPMSM. Still, unless high saliency ratio (L_d/L_q) and high inductance difference ($L_d - L_q$) are reached, torque density, power factor, and efficiency are low in the steady-state [4].

To increase L_d/L_q and $L_d - L_q$, the d-axis flux path should be obtained sufficiently. Consequently, q-axis conductor bars should be reduced.

In contrast, d-axis conductor bars should be increased to reduce the conductor bar loss by the unbalanced rotating magnetic field.

However, with flux barriers, the various shapes of the conductor bars can cause the unbalanced starting torque according to the initial starting position of the rotor. The starting torque is defined as the induction torque at zero speed in this paper.

This paper presents the design to improve the starting capability of the LSynRM.

The number and the shape of the conductor bars are set as design variables, and the starting performance with design variables

are analyzed by finite element method (FEM) [5].

The starting torque of a prototype and a designed model of the LSynRM are compared according to the initial starting position of the rotor.

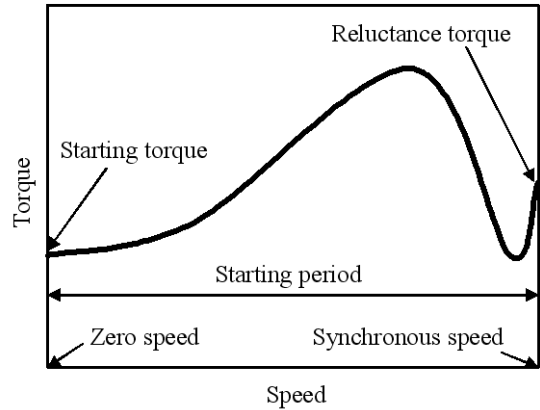


Figure 1. Torque vs. speed of LSynRM

II. LSYNRM DESIGN PROCEDURE

A. Decision of the Number of the Conductor Bars

In the case of the induction motor having the squirrel-cage rotor, the slot combination of the stator and the rotor affects the starting characteristics, even though the motor does not have the flux barriers. Therefore, it is very important to decide the number of the conductor bars.

Fig. 2 shows the analysis models according to the number of the conductor bars, which is 30, 32, 33, and 34, respectively.

It is assumed that the models have same magnetic material, shape, and dimension. The analysis models do not have flux barriers, and the conductor bar resistances are uniform to avoid the difference of the torque magnitude. The skew effect is not considered in this paper.

When the rotor positions in Fig. 2 are defined as initial starting position of zero, the FE analysis is performed from zero to eight with four-degree intervals.

Fig. 3 and Fig. 4 are FE analysis results of the starting torque with the number of the conductor bars and the initial starting position, when the speed is zero.

As shown in the figures, the starting torque with 30 and 32 bars varies severely, whereas the torque with 33 bars has almost uniform value.

The torque variation with 34 bars is smaller than that with 32 bars and is a little bit larger than that with 33 bars.

In the case of the LSynRM, an even number of the conductor bars is suitable because the motor requires the symmetric magnetic circuit. Thus, the rotor of the LSynRM has 34 bars in this paper.

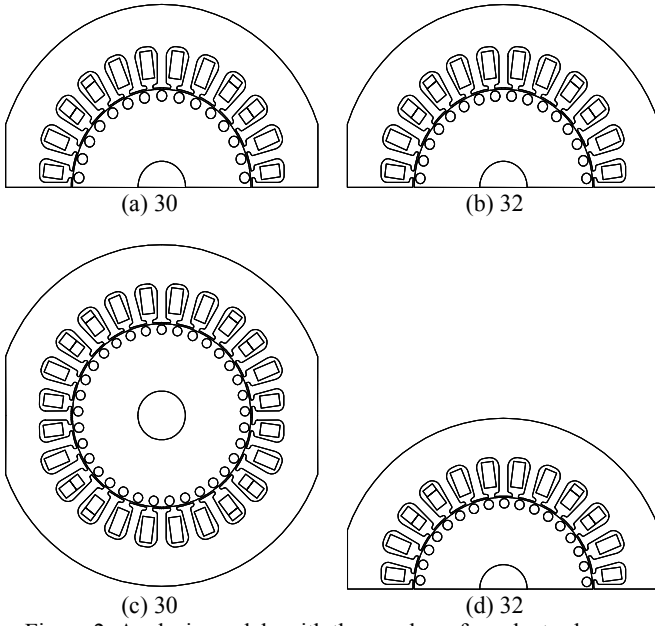


Figure 2. Analysis models with the number of conductor bars.

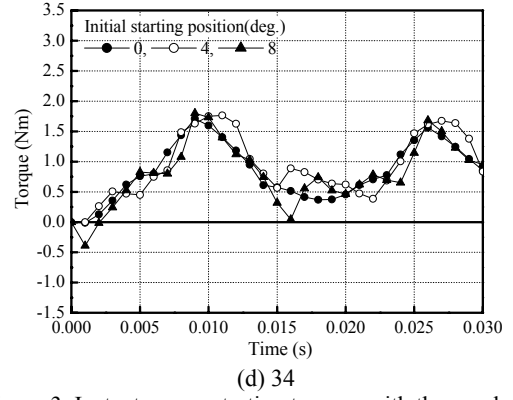
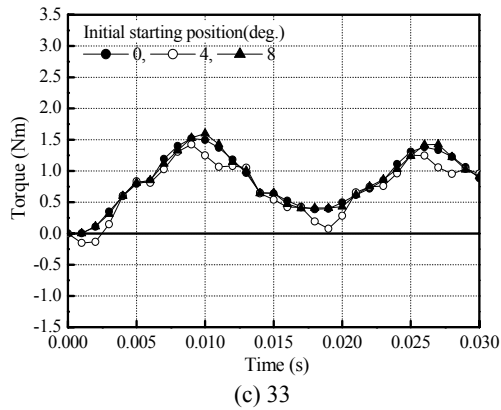
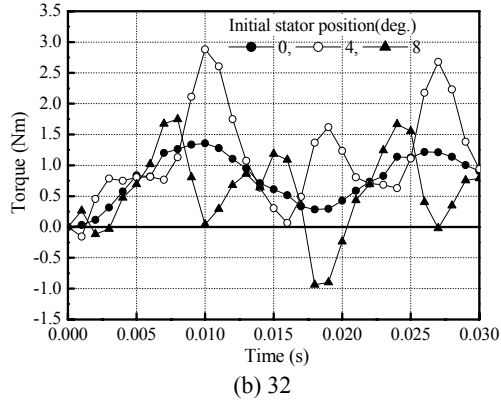
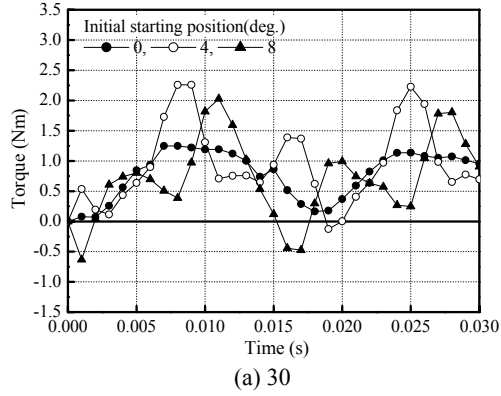


Figure 3. Instantaneous starting torques with the number of conductor bars and the initial rotor position at zero speed.

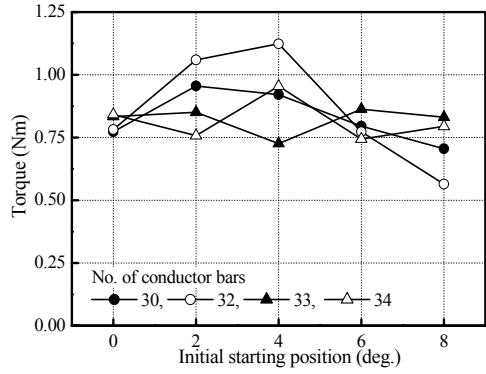


Figure 4. Average torques of the instantaneous starting torques in Fig. 3.

B. Torque Characteristics with the Shape of the Conductor Bars

Fig. 5 presents the analysis models having the various shapes of the conductor bars and the zero initial starting position.

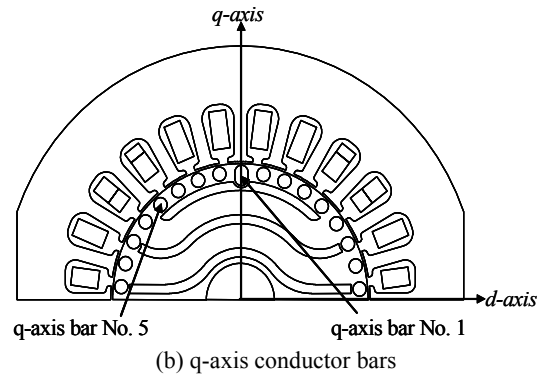
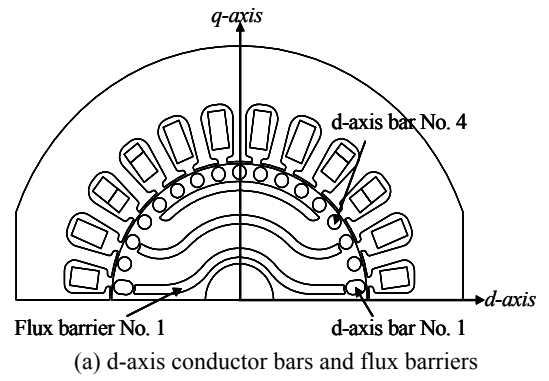


Figure 5. Analysis models with the shape of conductor bars.

The models have 34 conductor bars and 3 flux barriers. d-axis conductor bars are numbered from the center of d-axis in counterclockwise (CCW) direction. In the same manner, q-axis conductor bars are numbered from the center of q-axis in CCW direction. Flux barriers are numbered from the shaft in radial direction.

When the shape of the conductor bars varies in order, the motor does not have flux barriers. In other words, the motor operates as a SPIM. On the other hand, when the motor has flux barriers, conductor bars have equal shapes.

When the models have the same shape of the conductor bars without the flux barriers shown in Fig. 5, the average starting torques by FE analysis is shown in Fig. 6. The analysis is performed in ten-degree intervals from 0 deg. to 180 deg..

The torque, 0.65 Nm is normalized as 100 %.

As shown in Fig. 6, it is confirmed that the models, as induction motors, have a good self-start capability.

Fig. 7 displays the average starting torques with the shape of the conductor bars and the flux barriers.

From the left hand to the right hand, the values of the horizontal axis are named as Ref, Bard_1, Bard_2, Bard_3, Bard_4, Barq_1, Bar_q2, Barq_3, Barq_4, Barq_5, Barr_1, Barr_2, and Barr_3 in order. “Ref” means the SPIM which has uniform conductor bars. “Bard”, “Barq”, and “Barr” mean the d-axis bar, the q-axis bar, and the flux barrier, respectively. The area of the changed bar is twice larger than that of the original bar.

The values of the vertical axis are the normalized torque.

Provided that No. 1 of the d-axis bar is increased, the bar causes negative starting torque at 70 deg., even though the bar increases starting torque at that of 80 deg..

Contrary to the No. 1 of the d-axis bar, the increase of No. 2 of the d-axis bar induces negative starting torque at 80 deg., though the bar increases starting torque at the initial starting position of 70 deg..

When No. 2 of the q-axis bar is increased, the bar reduces the starting torque at 10 and 20 deg..

The flux barriers of No. 1 and No. 2 have an bad influence on the initial starting position of 70, 100, and 120 deg..

The rest of the conductor bars and the flux barriers also show the similar characteristics. Therefore, it is very important to design flux barriers, and, especially, conductor bars for a good starting performance from uniform starting torque with the initial starting position.

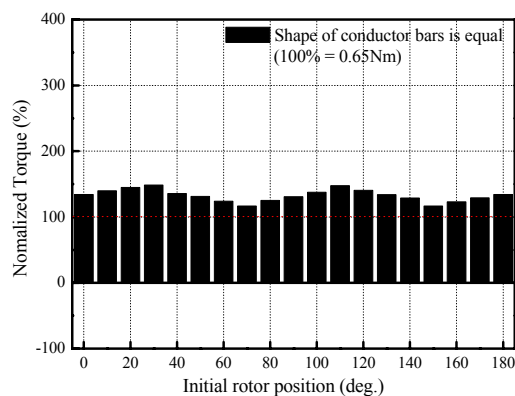
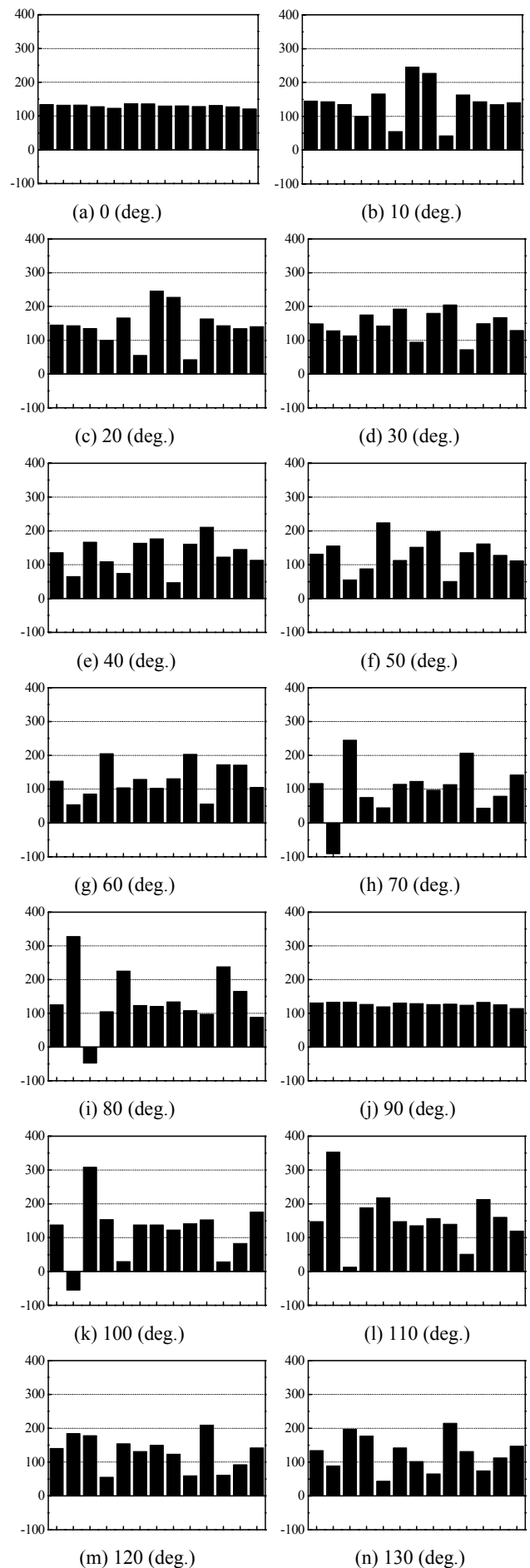


Figure 6. Average starting torques when the analysis models in Fig. 5 are operated as induction motors.



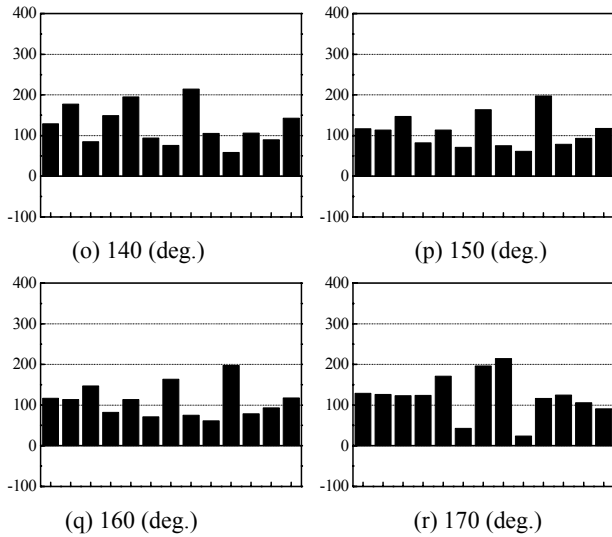


Figure 7. Analysis results of the average starting torque with the initial starting position

III. DESIGN RESULTS

Fig. 8 shows the cross-section of a prototype and a designed model of the LSynRM, respectively.

Two kinds of models have identical stators. The stator lamination, stack length, and winding's effective turns are the same. The rotors of the models are different. While the prototype has 32 bars and 5 flux barriers, the designed model has 34 bars and 3 flux barriers. The shapes of the conductor bar of the designed model are determined using Fig. 7.

Fig. 9 indicates average starting torques of the prototype and the designed model. In Fig. 9(a), the prototype has negative starting torque positions. Unlike this, the designed model generates positive starting torque all over the initial starting positions even though the starting torques between 30 deg. and 130 deg. are smaller than in other degrees.

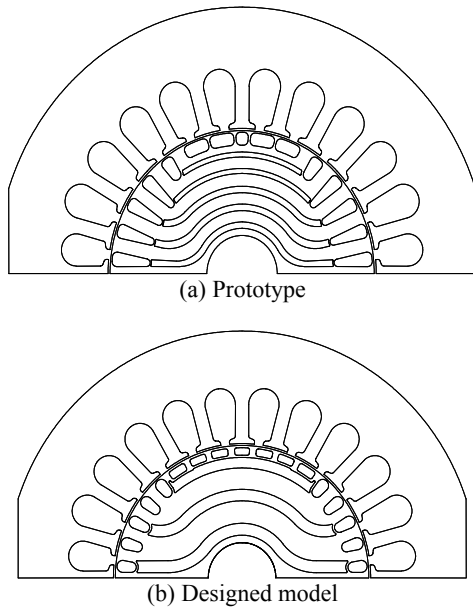
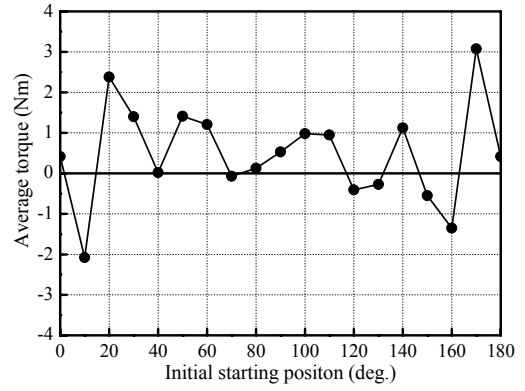
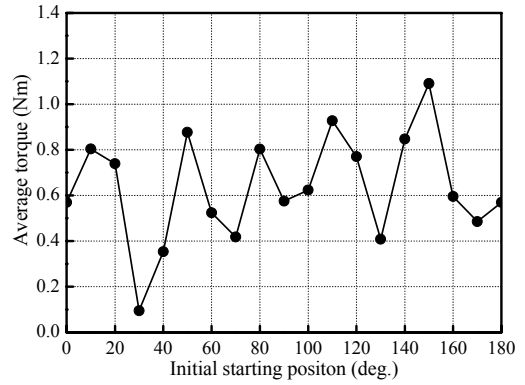


Figure 8. Cross-section of a prototype and a designed model of the LSynRM



(a) Prototype



(b) Designed model

Figure 9. Analysis results of the average starting torque of the prototype and the designed model.

IV. CONCLUSIONS

This paper deals with the LSynRM design to improve starting capability.

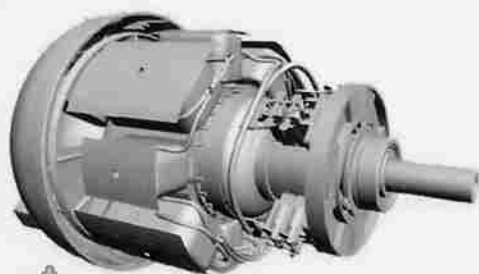
From the starting torque analysis results with the number of conductor bars, the number of 34 conductor bars is chosen for the LSynRM. In addition, the shape of the bar is decided to obtain the starting torque with the initial starting position.

It is confirmed that the designed model has a good self-start capability in comparison with the prototype.

V. REFERENCES

- [1] A. M. Knight, and C.I. McClay, "The design of high-efficiency line-start motors," in *Conf. Rec. the 34th IAS Annual Meeting*, vol. 1, pp. 516-522, Oct.1999.
- [2] G. H. Kang, J. Hur, H. Nam, J. P. Hong, and G. T. Kim, "Analysis of Irreversible Magnet Demagnetization in Line-Start Motors based on Finite Element Method," *IEEE Trans. Magn.*, vol.39, no.3, pp. 1488-1491, May 2003.
- [3] H. Murakami, Y. Honda, H. Kiriyaama, S. Morimoto, and Y. Takeda, "The performance comparison of SPMSM, IPMSM and SynRM in use as air-conditioning compressor," in *Conf. Rec. the 34th IAS Annual Meeting*, vol. 2, pp. 840-845, Oct.1999.
- [4] I. Boldea, Z. X. Fu, and S. A. Nasar, "Performance evaluation of axially-laminated anisotropic (ALA) rotor reluctance synchronous motors," *IEEE Trans. Ind. Applicat.*, vol.30, no.4, pp. 977-985, July/August 2003.
- [5] H. Kiriyaama, S. Kawano, Y. Honda, T. Higaki, S. Morimoto, and Y. Takeda, "High performance synchronous reluctance motor with multi-flux barrier for the appliance industry," in *Conf. Rec. the 33th IAS Annual Meeting*, vol. 1, pp. 111-117, Oct.1998.

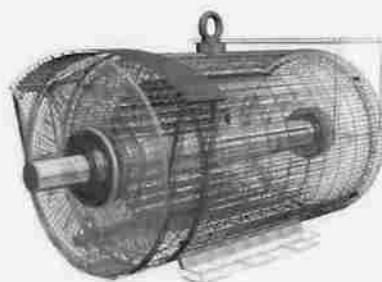
16th International Conference on Electrical Machines



ICEM 2004



5-8 SEPTEMBER 2004, CRACOW - POLAND



BOOK OF DIGESTS

vol 1

Editors: S. Wiak, M. Dems, K. Komeza



Institute of Mechatronics and Information Systems
Technical University of Lodz, Poland

PS2-21	Fractional-Slot IPM Servomotors: Analysis and Performance Comparisons.....	173
	<i>N. Bianchi, S. Bolognani, G. Grezzani</i>	
PS2-22	Electric Motors Featuring Multiple Degrees-of-Freedom	175
	<i>P. Bolognesi, O. Bruno, A. Landi, L. Sani, L. Taponecco</i>	
PS2-23	Performance Analysis of a Solid Rotor Disk Induction Motor	177
	<i>S.E. Abdollahi, M. Mirsalim, M. Mirzayee</i>	
PS2-24	Increase Armature Voltage for the Superconducting DC Motor.....	179
	<i>D. Wu, J. Chen</i>	
PS2-25	Low-Stiffness Motor: Review of Different Ironless Motors Topologies for Use in Precision Engineering Applications.....	181
	<i>M.H. El-Husseini, J.W. Spronck, H. Polinder, H.H. Langen, J. van Eijk</i>	
PS2-26	Design to Improve Starting Capability of Single-Phase Line-Start Synchronous Reluctance Motor ...	183
	<i>Hyuk Nam, Su-Beom Park, Jung-Pyo Hong, Tae-Uk Jung, Jae-Boo Eom</i>	
PS2-27	Optimal Design for Volume Reduction of Nd-Fe-B Magnet in BLDC Motor	185
	<i>Sang-Joon Han, Hong-Soon Choi, Il-Han Park</i>	
PS2-28	New Development of Multifunction Device for 4 Different Functions in Mobile Phones	187
	<i>Sang-Moon Hwang, Hong-Joo Lee, Keum-Shik Hong, Beom-Soo Kang, Gun-Yong Hwang</i>	
PS2-29	Magnetic Barrier Effect on Operating Performances of Switched Reluctance Motor	189
	<i>J.Y. Lee, K.Y. Nam, Jung-Pyo Hong, J. Hur</i>	
PS2-30	Steady State Model of the Single-Phase Capacitor-Run Hybrid Induction Motor	191
	<i>Sun-Ki Hong</i>	
PS2-31	Simulation and Experimentation of a Two-Phase Claw-Pole Motor	193
	<i>A. Reınap, M. Alaküla</i>	
PS2-32	New Design of Switched Reluctance Motor to Improve ITS Efficiency	195
	<i>P. Rafajdus, V. Hrabovcová, M. Lipták, I. Zrak</i>	
PS2-33	Induction Motors with Spherical Rotor	197
	<i>G. Kamiński, A. Smak</i>	
PS2-34	Design and Optimisation of Brushless Integrated Starter-Generator	199
	<i>L. Gašparin, R. Fišer</i>	
PS2-35	Simulation and Experimentation of a Single-Phase Claw-Pole Motor	201
	<i>A. Reınap, M. Alaküla, G. Nord, L.O. Hultman</i>	
PS2-36	Optimal Excitation Parameters of a Single-Phase SR Generator.....	203
	<i>M. Lipták, P. Rafajdus, V. Hrabovcová, I. Zrak</i>	
PS2-37	Comparison of Brushless DC Motors with Concentrated Winding and Segmented Stator.....	205
	<i>J. Cros, P. Viarouge, R. Carlson, L.V. Dokonal</i>	

vol 2

Special Machines

OS4

OS4-1	Design of a High Speed Permanent Magnet Brushless Generator for Microturbines	209
	<i>J.F. Gieras</i>	
OS4-2	Variable Pole, Variable Phase Machines	211
	<i>M. McCulloch</i>	
OS4-3	Asynchronous Wheel Hub Motor with Massive Rotor Iron and Open Rotor Slots for Wheel Hub Drives in Street Cars	213
	<i>W. Hackmann, A. Binder</i>	
OS4-4	Control of Switched Reluctance Machines for Flywheel Energy Storage Applications	215
	<i>M. Holub, R. Palka, W.R. Canders</i>	
OS4-5	Study on Magnetic Field and Output Voltage of Axial Type Generator for Wind Power Generation ...	217
	<i>E. Mukai, S. Washimiya</i>	
OS4-6	Electrostatic Synchronous Motors.....	219
	<i>M. Crivii, M. Jufer</i>	